

Secondary Amides of Sulfonylated 3-Amidinophenylalanine. New Potent and Selective Inhibitors of Matriptase[†]

Torsten Steinmetzer,^{*,‡} Andrea Schweinitz,[‡] Anne Stürzebecher,[‡] Daniel Dönnecke,[‡] Kerstin Uhland,[‡] Oliver Schuster,[‡] Peter Steinmetzer,[§] Friedemann Müller,[‡] Rainer Friedrich,[#] Manuel E. Than,^{#,||} Wolfram Bode,^{#,||} and Jörg Stürzebecher[§]

Curacyte Chemistry GmbH, Winzerlaer Strasse 2, D-07745 Jena, Germany, Curacyte Discovery GmbH, Deutscher Platz 5d, D-04103 Leipzig, Germany, Institut für Vaskuläre Medizin, Klinikum der Universität Jena, Nordhäuser Strasse 78, D-99089 Erfurt, Germany, Max-Planck-Institut für Biochemie, Forschungsgruppe Proteinase, Am Klopferspitz 18, D-82152 Martinsried, Germany, and Ludwig-Maximilians-Universität München, Department of Chemistry and Biochemistry, Genzentrum, Feodor-Lynen-Strasse 25, 81377 München, Germany

Received December 21, 2005

Matriptase is an epithelium-derived type II transmembrane serine protease and has been implicated in the activation of substrates such as pro-HGF/SF and pro-uPA, which are likely involved in tumor progression and metastasis. Through screening, we have identified bis-basic secondary amides of sulfonylated 3-amidinophenylalanine as matriptase inhibitors. X-ray analyses of analogues **8** and **31** in complex with matriptase revealed that these inhibitors occupy, in addition to part of the previously described S4-binding site, the cleft formed by the molecular surface and the unique 60 loop of matriptase. Therefore, optimization of the inhibitors included the incorporation of appropriate sulfonyl substituents that could improve binding of these inhibitors into both characteristic matriptase subsites. The most potent derivatives inhibit matriptase highly selective with K_i values below 5 nM. Molecular modeling revealed that their improved affinity results from interaction with the S4 site of matriptase. Analogues **8** and **59** were studied in an orthotopic xenograft mouse model of prostate cancer. Compared to control, both inhibitors reduced tumor growth, as well as tumor dissemination.

Introduction

Cancer is a leading cause of mortality worldwide. Although single tumors can often be removed by surgery or treated with chemotherapy or radiotherapy, the patients often die because of formation of metastases. Metastasis formation includes complex processes, which also require a series of proteolytic steps for degradation and remodeling of the extracellular matrix. After penetration through the basal lamina around the primary tumor, which mainly consists of collagen, glycoproteins, and proteoglycans, the tumor cells have to migrate through extracellular matrix proteins in the connective tissue and intravasate through a basal membrane into the blood or lymph system. After distribution over the whole body, tumor cells extravasate from the vascular system and form metastases at different loci. Proteases of different families, such as matrix metalloproteases and aspartate, cysteine, and serine proteases, are implicated in these processes and are also responsible for growth factor activation and angiogenesis, which are required for normal tumor growth and progression. Therefore, the development of specific inhibitors for these proteases is one possible strategy to prevent metastasis. During the past decade, extensive work has focused on the development of inhibitors for matrix metalloproteases (MMP). However, all clinical cancer trials with relatively nonspecific MMP inhibitors showed only poor efficacy.¹ In addition, the urokinase-type plasminogen activator (uPA), a serine protease of the plasmin/plasminogen activator system, emerged as a potential target for antimetastatic drugs.^{2,3} The

tumor-associated serine proteases of the plasmin/plasminogen activator system and matrix metalloproteases are closely connected in a proteolytic cascade. uPA is assigned to be the major activator of plasmin, which in turn generates more uPA in a feedback reaction and also activates MMPs, which are responsible for the degradation of extracellular matrix proteins.

The zymogen pro-uPA can also be activated in vitro by several proteases other than plasmin, among them the cysteine proteases cathepsin B and cathepsin L, the aspartate protease cathepsin D, and the trypsin-like serine proteases plasma kallikrein, prostate-specific antigen or tryptase. Recently, it was also shown that matriptase, an epithelial-derived type II transmembrane serine protease,⁴ converts pro-uPA into enzymatically active uPA with high efficacy.⁵ In addition, matriptase is a very potent activator of hepatocyte growth factor (HGF, also named scatter factor), which acts as a major motility factor and induces scattering of cells through binding and activation of its cell surface receptor c-Met. A preferred cleavage sequence of matriptase also contains the protease-activated receptor-2 (PAR2), and it has been shown that a soluble form of matriptase can trigger calcium signaling from PAR2-expressing *Xenopus* oocytes.⁵

Enzymatically active matriptase was originally isolated from human breast cancer cells^{7,8} and in an inhibited form through binding to endogenous hepatocyte growth factor activator inhibitor-1 (HAI-1) from human milk.⁹ Independently, it was cloned as MT-SP1 (membrane-type serine protease 1) from a human prostatic cancer cell line.¹⁰ Matriptase (76 kDa) has a reduced size when compared with MT-SP1 (95 kDa) because of a truncation in the integral N-terminal anchor peptide. However, the catalytic serine protease domain of both enzymes is identical. Recently, the crystal structures of this catalytic domain in complex with the small inhibitor benzamidine and with the bovine pancreatic trypsin inhibitor have been published.¹¹

Matriptase emerged as a potential target for the development of anti-invasiveness drugs to prevent metastasis due to its

[†] Coordinates of **8**/matriptase and **31**/matriptase have been deposited to the Protein Data Bank under PDB codes 2gv6 and 2gv7, respectively, and will be released upon publication of the manuscript.

* To whom correspondence should be addressed. Telephone: +49-3641-508516. Fax: +49-3641-508507. E-mail: torsten.steinmetzer@curacyte.com.

[‡] Curacyte Chemistry GmbH.

[§] Curacyte Discovery GmbH.

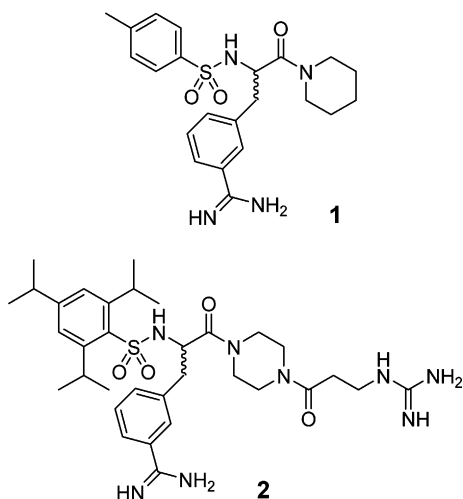
[§] Klinikum der Universität Jena.

[#] Max-Planck-Institut für Biochemie, Forschungsgruppe Proteinase.

^{||} Ludwig-Maximilians-Universität München.

potential substrates pro-uPA and pro-HGF and due to its overexpression in epithelial tumors.^{12–14} Recently it was demonstrated that a modest orthotopic overexpression of matriptase in transgenic mice caused spontaneous squamous cell carcinoma and potentiated carcinogen-induced tumor formation, whereas increased expression of HAI-1 completely negated the oncogenic effects of matriptase.¹⁵ Presently, only a few matriptase inhibitors have been described, among them several bis-benzamides with inhibition constants between 0.1 and 1 μM ¹⁶ and a 14-amino acid peptide isolated from sunflower seeds having a K_i value of 0.92 nM.¹⁷ Recently, a selective arginal-derived matriptase inhibitor (CVS-3983, $K_i = 3.3$ nM) has been used to suppress the growth of androgen-independent prostate tumor xenografts.¹⁸

One of the archetypical inhibitors of almost all trypsin-like serine proteases is 3-TAPAP (**1**),¹⁹ which also inhibits matriptase with an inhibition constant of 14 μM . A thorough screening of other available sulfonylated 3-amidinophenylalanine derivatives led to the identification of racemic compound **2** from a previously described series of uPA inhibitors.²⁰ Compound **2** has a K_i value of 82 nM for matriptase and reduced affinity toward related trypsin-like serine proteases, such as the clotting proteases thrombin and factor Xa or the fibrinolytic enzymes plasmin and uPA.

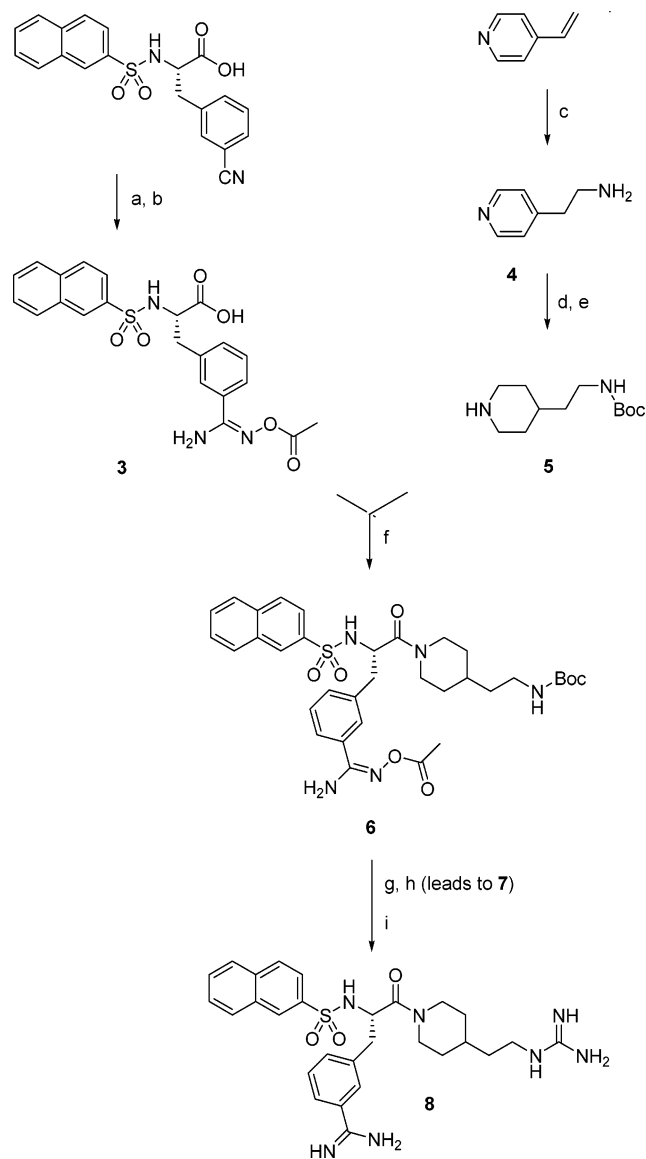


For further optimization of inhibitor **2**, we maintained the central 3-amidinophenylalanine as a key moiety and modified the N-terminal sulfonyl group and the C-terminal secondary amide residue. These modifications resulted in a series of new compounds, which show improved potency and selectivity as matriptase inhibitors. Two analogues were selected for X-ray analysis in complex with the catalytic domain of matriptase to obtain information about their binding mode. This structural information was used for further inhibitor design. In addition, two inhibitors were investigated for their anti-invasive potential and inhibition of tumor growth in an orthotopic xenograft mouse model of prostate cancer. The results are summarized in this publication.

Results

Chemistry. The compounds were synthesized according to published procedures. Scheme 1 exemplarily summarizes the synthesis of inhibitor **8**. The cyano group of an appropriate sulfonylated 3-cyanophenylalanine was converted into an acetylated hydroxyamidino **3** by the method of Judkins.²¹ The C-terminal part of the molecule was obtained from 4-vinylpyridine as starting material. Treatment with ammonium chloride

Scheme 1. Synthesis of Inhibitor **8**^a

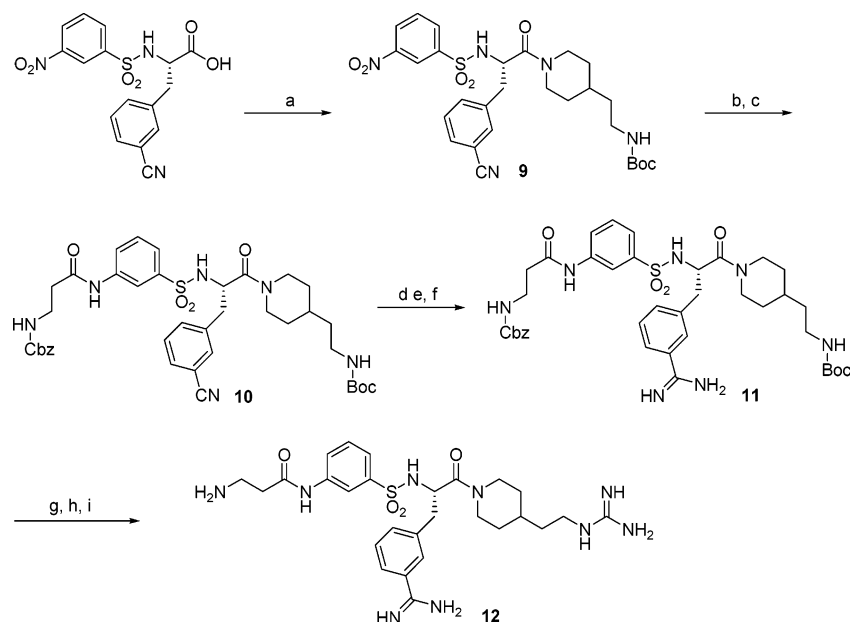


^a Reagents and conditions: (a) 2.0 equiv of $\text{NH}_2\text{OH}\cdot\text{HCl}$ and DIPEA in ethanol; (b) 2 equiv of $(\text{Ac})_2\text{O}$ in acetic acid; (c) 2 equiv of NH_4Cl in water/methanol; (d) $(\text{Boc})_2\text{O}$ in ethyl acetate; (e) H_2 and PtO_2 as catalyst in 90% acetic acid; (f) PyBop/DIPEA in DMF; (g) 1 N HCl in acetic acid; (h) H_2 and Pd/C in 90% acetic acid; (i) 1.5 equiv of 1H-pyrazole-1-carboxamide·HCl/DIPEA in DMF, preparative reversed-phase HPLC.

led to 4-aminoethylpyridine **4**,^{22,23} which was Boc-protected and hydrogenated using platinum(IV) oxide as catalyst to give intermediate **5**. Coupling of **3** and **5** using PyBop/diisopropylethylamine resulted in **6**. The intermediate obtained after Boc cleavage was hydrogenated and treated with pyrazole-1-carboxamide²⁴ to give inhibitor **8**.

Inhibitors containing a phenoxyarylsulfonyl group (**53**, **54**) were obtained alternatively by reduction of the appropriate acetylhydroxyamidino derivative with zinc powder in acetic acid (3 h, room temperature), because of the instability of such sulfonyl residues under catalytic hydrogenation conditions using Pd/C as catalyst.

Inhibitors **56–63** were obtained by mixed-anhydride-mediated coupling of Boc- or Cbz- β -Ala-OH and its glycine and γ -aminobutyric acid analogues to 3- or 4-aminobenzenesulfonyl-3-cyanophenylalanyl-(Boc-amidoethyl)piperidine, which was obtained by reduction of the appropriate nitrobenzenesulfonyl derivative with zinc powder in acetic acid. For compounds **62**

Scheme 2. Synthesis of Inhibitor **12**^a

^a Reagents and conditions: (a) compound **5** and PyBop/DIPEA in DMF; (b) zinc powder in acetic acid, 2 h, room temp; (c) Cbz- β -Ala-OH, isobutyl chloroformate, *N*-methylmorpholin in DMF; (d) 2 equiv of $\text{NH}_2\text{OH}\cdot\text{HCl}$ and DIPEA in ethanol; (e) 2 equiv of $(\text{Ac})_2\text{O}$ in acetic acid; (f) zinc powder in acetic acid, 3 h, room temp; (g) 90% TFA, 1 h, room temp; (h) 1.5 equiv of 1*H*-pyrazole-1-carboxamide·HCl/DIPEA in DMF; (i) H_2 and Pd/C in 90% acetic acid, preparative reversed-phase HPLC.

and **63** the appropriate Boc-amidopropylpiperidide derivative was used. The nitrile moiety was converted into an amidine by the procedures described in Scheme 1 for all compounds with identical *N*- and *C*-terminal amino or guanidino groups (e.g., **59** and **58**). In contrast, the acetylhydroxyamidino group was converted to the amidine using zinc powder in acetic acid (3 h, room temperature) for inhibitors with a single *C*-terminal guanidino group (**12** and **63**). This strategy retained the *N*-terminal Cbz protection and allowed the selective guanylation of the *C*-terminus using pyrazole-1-carboxamide²⁴ as shown in Scheme 2 for the synthesis of inhibitor **12**.

Enzyme Kinetics and X-ray Crystallography. To elucidate the binding geometry of compound **2**, we superimposed the known X-ray structure of uPA with compound **13** (PDB code 1F92),²⁵ which is closely related to **2**, using the matriptase structure as deposited under the PDB entry 1EAX.¹¹ On the basis of this model, we hypothesized that the *C*-terminal guanidino group of inhibitor **2** might interact with the superficial, solvent-exposed side chain of matriptase residue Asp96 (chymotrypsinogen numbering¹¹), which is harbored in the 99 loop “balcony” delimiting the active-site cleft to the north and extends toward the S2 subsite. To probe this interaction, further analogues of **2** with variable lengths of the guanidinoalkyl chain and different hydrophobic sulfonyl residues were prepared. Their affinity was measured toward matriptase and the closely related clotting proteases thrombin and factor Xa as well as toward the fibrinolytic enzymes plasmin and uPA.

Most of the inhibitors summarized in Table 1 show a preference for matriptase over the other enzymes. In analogy to known uPA or thrombin inhibitors, the affinity of racemic **2** could be improved by using 3-amidinophenylalanine in the *S*-configuration (**2S**). Inhibitors with a *C*-terminal guanidino group have been found to be 2–3 times more potent than the analogous amino derivatives in most cases. There is only a marginal difference in matriptase affinity between compounds **2S** and **14**, containing a guanidinopropionyl or butyryl group, respectively. A slightly enhanced potency toward matriptase was observed after incorporation of a cyclic *N*-(amidino)isonipecotyl

residue (**31**). In contrast, the exchange of the piperazine ring by homopiperazine has a negligible effect on the inhibition of matriptase (e.g., inhibitor **13** vs **19**, and **2S** vs **18**).

The elimination of the basic group in the *C*-terminal part of the molecule (**35**, **36**) reduces the potency toward matriptase. However, the previously described nonselective uPA inhibitor **35** (WX-UK1), containing a neutral ethyloxycarbonyl group, still inhibits matriptase with an inhibition constant of 0.32 μM , which is comparable to the inhibition value toward uPA.²⁶ Some of the described effects of **35** in suppression of rat breast cancer metastasis and tumor growth reduction could also possibly be related to matriptase inhibition.

In previous work with closely related thrombin inhibitors containing a central 3-amidinophenylalanylpiperazide, it was found that the piperazine moiety could be replaced by other secondary amines, among them isonipecotic acid.^{27,28} Therefore, isonipecotic acid analogues were synthesized, which allow for a simple *C*-terminal elongation with basic residues derived from diaminoethane or piperazine (Table 2).

The incorporation of isonipecotic acid resulted in selective and potent matriptase inhibitors. Also in this series, compounds containing a *C*-terminal guanidino moiety were more potent than the corresponding amino analogues. In contrast to the piperazine derivatives (Table 1), the 2,4,6-triisopropylphenylsulfonyl derivatives are less effective than the anthraquinonesulfonyl- or 4-cyclohexylphenylsulfonyl analogues. Only small differences in matriptase affinity were found after replacement of the *C*-terminal alkylguanidino group by a cyclic carbamidoylpiperazine. In an additional series, more simple bis-basic secondary amines were incorporated to eliminate one of the peptide bonds in these molecules. The kinetic results are summarized in Table 3.

Several inhibitors (**8**, **50**, **52**) inhibit matriptase with K_i values of approximately 50 nM and maintain some selectivity toward the other enzymes. To obtain information of the binding mode, two inhibitors (**8**, **31**) were selected for X-ray analysis. Figure 1 shows the complex between matriptase and these inhibitors. Some characteristic interactions are very similar in both structures. The inhibitors adopt a compact Y-shaped conforma-

Table 1. Inhibition Constants for Inhibitors of the General Compound Shown^a

No.	R	R ₁	n	K _i (μM)					No.	R	R ₁	n	K _i (μM)				
				matriptase	uPA	plasmin	thrombin	fXa					matriptase	uPA	plasmin	thrombin	fXa
2S			1	0.057	0.82	1.4	1.6	2.9	25			1	0.25	4.0	3.1	0.58	10
13			1	0.17	0.64	0.44	3.3	15	26			1	0.34	19	3.7	2.5	5.1
14			1	0.061	0.26	0.88	4.2	2.8	27			1	0.40	43	12	2.6	130
15			1	0.14	1.1	0.64	9.4	13	28			1	0.69	56	4.2	1.5	80
16*			1	0.33	1.5	0.82	1.2	9	29			1	0.73	25	10.2	3.0	>1000
17*			1	0.69	8.9	3.4	0.20	10.5	30			1	0.10	1.2	1.3	5.4	17
18			2	0.065	0.81	0.44	0.62	1.2	31			1	0.014	1.1	0.60	5.0	10
19			2	0.096	1.2	0.36	0.49	5.3	32			1	0.061	12	1.4	1.3	2.8
20			1	0.053	26	7.2	1.8	2.8	33			2	0.13	2.5	0.26	5.0	5.8
21			1	0.044	6.1	3.2	0.46	4.6	34			2	0.050	4.6	0.33	2.5	4.1
22			1	0.089	10.5	0.78	0.12	2.3	35			1	0.32	0.41	0.39	0.49	1.7
23			1	0.20	18	2.5	0.26	8.3	36			1	1.5	31	6.0	0.054	1.3
24			1	0.21	6.9	2.8	1.4	56									

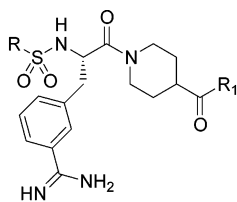
^a The asterisk (*) indicates that the compound is racemic at the C_α-atom of 3-amidinophenylalanine.

tion similar to that previously found for related arylsulfonyl-3-amidinophenylalanine-derived inhibitors in complex with uPA, thrombin, or trypsin.^{25,29,30} The central benzamidine moiety is sandwiched, like the free benzamidine,¹¹ between matriptase segments Ser190-Gln192 and Trp215-Gly216. The two amidino nitrogens juxtapose the two carboxylate oxygens of Asp189 situated at the bottom of the S1 specificity pocket under formation of favorable twin ionic bonds and form additional hydrogen bonds to the carbonyl of Gly219, the side chain hydroxyl of Ser190, and a conserved water molecule.

The 3-amidinophenylalanyl moiety is positioned, similar to that found in the complexes of inhibitor **1** in trypsin³¹ and inhibitor **13** in uPA,²⁵ such that its NH and carbonyl groups form hydrogen bonds to the carbonyl and the NH group of Gly216, respectively. In addition, one of the two sulfonamide

oxygens is in hydrogen bond distance to Gly219 NH. In both structures, the sulfonated aryl ring and the proximal piperidyl or piperazine group are folded together into a compact entity, making intense contacts with the hydrophobic cleft formed by Trp215, the His57 imidazole ring, and the Phe99 phenyl group. Presumably, this conformation is close to the preferred conformation in solution, resulting in improved binding due to entropically favorable conditions.²⁹

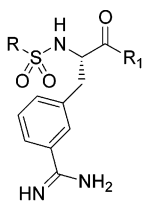
The piperidine group of compound **8**, on the C-terminal side, can adopt both a boat and a chair conformation, with the equatorial guanidinoethyl group extending into the negatively charged "cation cleft" formed by the initial part of the characteristically exposed 60 insertion loop and the active-site cleft of matriptase and lined by the Asp96 carboxylate, the carbonyl groups of His57 and Ile60, and the carboxylate group

Table 2. Inhibition Constants for Isonipecotic Acid Containing Inhibitors of the General Compound Shown


No.	R	R ₁	K _i (μM)				
			matriptase	uPA	plasmin	thrombin	FXa
37			0.38	1.2	0.94	16	6.3
38			0.14	0.62	1.8	20	5.0
39			0.021	7.7	3.1	0.42	4.0
40			0.013	3.6	4.1	0.42	4.9
41			0.10	0.87	0.80	1.3	4.6
42			0.084	1.6	1.8	13	3.7
43			0.24	6.6	2.8	0.17	1.1
44			0.026	8.2	3.1	1.7	1.3

of Asp60b. With some of these hydrogen bond acceptors, the guanidyl group makes water-mediated hydrogen bonds. The N-terminal naphthyl moiety of inhibitor **8** is, in contrast to the equivalent naphthyl group of NAPAMP-thrombin,²⁹ curiously abductant from the active-site cleft, making only weak van der Waals contacts with Trp215. This might be due to a concerted movement done together with the C-terminal moiety but might also be caused by the Arg60c side chain of a symmetry-related matriptase molecule extending into the S4 subsite. Both the proximal piperazine and the distal piperidine group, located on the C-terminal side of compound **31**, are confined to the chair conformation. The distal amidino group extends into the aforementioned “cation cleft”, making hydrogen bonds with Ile60 O (strong), Asp60a, and Cys58 O (weak). The triisopropylphenylsulfonyl group of inhibitor **31**, on the N-terminal side, is, as in the urokinase complex with the closely related inhibitor **13**,²⁵ abductant from the active-site cleft, making only a weak contact with Trp215 via one isopropyl group. Again, this loose contact might in part be due to the extending Arg60c side chain of a neighboring matriptase molecule.

Therefore, in solution, the N-terminal sulfonyl groups might further approach the S2/S4 subsite and extend into the hydrophobic surface cleft formed by the side chains of Phe97, Phe99, Gln175, and Trp215 and by the carbonyl groups of Phe97 and Thr98 of matriptase. Molecular modeling revealed that it might be possible to use this binding site of matriptase by incorporation of appropriate sulfonyl substituents. Kinetic results for the first derivatives of this type are summarized in Table 4, showing that several inhibitors have improved affinity and selectivity toward matriptase.

Table 3. Inhibition Constants for Inhibitors of the General Compound Shown


No.	R	R ₁	K _i (μM)				
			matriptase	uPA	plasmin	thrombin	FXa
45			0.11	2.3	1.4	0.21	76
8			0.046	1.3	20	0.11	27
46			0.072	2.3	1.7	0.19	13
47			0.088	1.9	2.0	0.051	1.8
48			0.089	0.32	1.0	0.30	3.2
49			0.16	2.1	0.73	0.6	66
50			0.042	2.1	1.2	0.17	34
51			0.12	2.2	0.21	12	24
52			0.045	1.3	1.4	1.8	25

Orthotopic Xenograft Mouse Model of Prostate Cancer.

A nonselective macromolecular inhibitor of matriptase, the serine protease inhibitor ecotin, has previously been reported to inhibit the growth and dissemination of tumors derived from the matriptase-expressing human prostate cancer cell line PC-3 in immune-compromised mice.¹⁰ The anti-invasive potential of the matriptase inhibitors **8** and **44** on PC-3 cells was previously demonstrated in an in vitro scatter assay.³² To detect the anti-invasive activity of the matriptase inhibitors in vivo as well, we investigated the effects of the initial lead compound **8** and the more potent and more selective derivative **59** on tumor growth and metastasis formation in nude mice bearing orthotopically implanted PC-3 prostate carcinoma. The inhibitors were administered intraperitoneally at a daily dose of 5 mg/kg for 4 weeks to nude mice with established orthotopic prostate tumors that were transplanted from the invasive part of human PC-3 tumor tissue pregrown subcutaneously in nude mice. The inhibitors **8** and **59** were both well tolerated by the PC-3 tumor-bearing mice and reduced the median primary tumor growth by 17% and 40%, respectively, compared to a vehicle-treated control group (Figure 2A).

In addition, the inhibitors further reduced substantially metastasis formation. Whereas 30% of the control mice had metastases in the thorax (heart, lung, pleura), metastases were only found in 14% and 20% of the thoraxes of the animals treated with compounds **8** and **59**, respectively. The effect was even more pronounced with abdominal metastases. Whereas metastases were found in 50% of the abdomens of the control mice, abdominal metastasis formation was completely abolished in both of the treatment groups (Figure 2B). These results

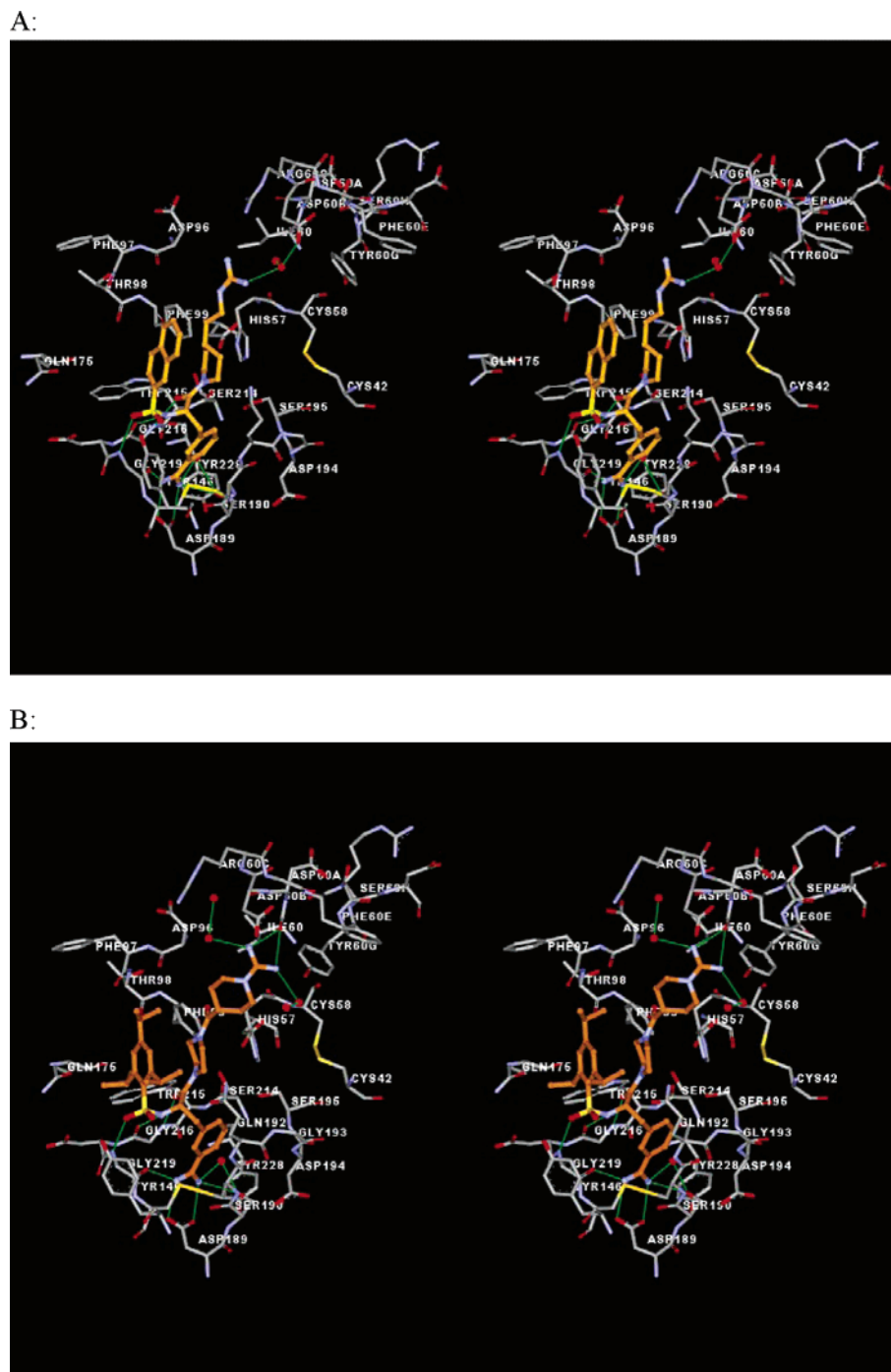


Figure 1. Stereoview of inhibitors **8** (A) and **31** (B) bound to the active site of matriptase. Selected matriptase residues are labeled, and strong hydrogen bonds are shown in green. Only water molecules that are involved in strong hydrogen bonding are shown (red balls).

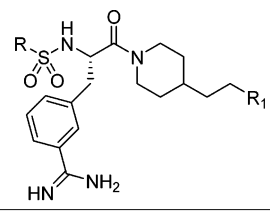
indicate that matriptase might be a relevant target in the progression of prostate cancer.

Discussion

Several series of matriptase inhibitors based on secondary amides of 3-amidinophenylalanine have been developed. Their structures are closely related to previously described thrombin or urokinase inhibitors of the 3-amidinophenylalanine type.^{20,28} In contrast to these compounds, however, the matriptase inhibitors presented in this study contain an additional basic group in the C-terminal part of the molecule, which is important for selectivity and contributes to potency. The replacement of the basic acylated piperazide segment, used for all compounds summarized in Table 1, by simple basic alkylpiperidines

(compounds shown in Tables 3 and 4) was well tolerated. Although the elimination of a peptide bond should increase their conformational flexibility, which often leads to less potent derivatives, this was not the case for these matriptase inhibitors.

Originally, we had assumed that the C-terminal basic group interacts with the side chain of the matriptase residue Asp96. However, in both X-ray crystal structures the C-terminal distal guanidyl group is directed into the aforementioned "cation cleft" between the initial 60 insertion loop and the matriptase surface rather than to the relatively flexible Asp96 side chain carboxylate, which is placed at the outer edge of this hole. The outward location of the N-terminal arylsulfonyl groups, in contrast, might be an artifact of the distinct matriptase crystal packing. We speculate that in solution the arylsulfonyl groups might be placed

Table 4. Inhibition Constants for Inhibitors of the General Compound Shown


No.	R	R ₁	K _i (μM)				
			matriptase	uPA	plasmin	thrombin	fXa
53			0.038	2.3	0.76	0.21	1.0
54			0.013	3.4	1.4	0.099	2.2
55			0.053	3.6	0.84	0.27	2.3
56			0.0087	0.60	1.2	1.8	10
57			0.028	0.82	1.2	8.8	15
58			0.0042	1.2	1.8	4.0	2.0
12			0.0018	1.7	5.0	6.0	9.5
59			0.0066	3.6	2.4	27	21
60			0.0039	8.0	2.5	21	23
61			0.075	11	4.5	7.0	35
62			0.005	1.5	2.7	13	15
63			0.0015	1.8	2.8	4.0	13

closer to the S4 subsite and nestle into the hydrophobic S2/S4 cleft of matriptase.

Therefore, inhibitors were synthesized that contain an aryl ring bridged via an oxygen or methylene to the para position of an arylsulfonyl group or that possessed an additional acyl residue attached to the aryl moiety via a peptide bond. Several of these inhibitors have enhanced matriptase affinity and improved selectivity (see Table 4). Molecular modeling in complex with matriptase revealed that the terminal phenoxy ring of inhibitor **54** and the β-Ala moiety of compound **59** may occupy the S4-binding site of matriptase (Figure 3).

The binding mode of inhibitor **59** may explain its improved affinity and selectivity as matriptase inhibitor. As suggested previously, the S4 subsite of matriptase seems to be well suited to accommodate residues containing positively charged groups.^{5,11}

To detect potential side effects for in vivo testing, selected matriptase inhibitors **8**, **54**, **59**, and **63** were evaluated for their influence on blood clotting. The very specific matriptase inhibitors **59** and **63** did not show any significant activity (IC₂₀₀ > 10 μM) in the standard coagulation assays, such as activated partial thromboplastin time (aPTT), prothrombin time (PT), and thrombin time (TT). In contrast, some anticoagulant activity was

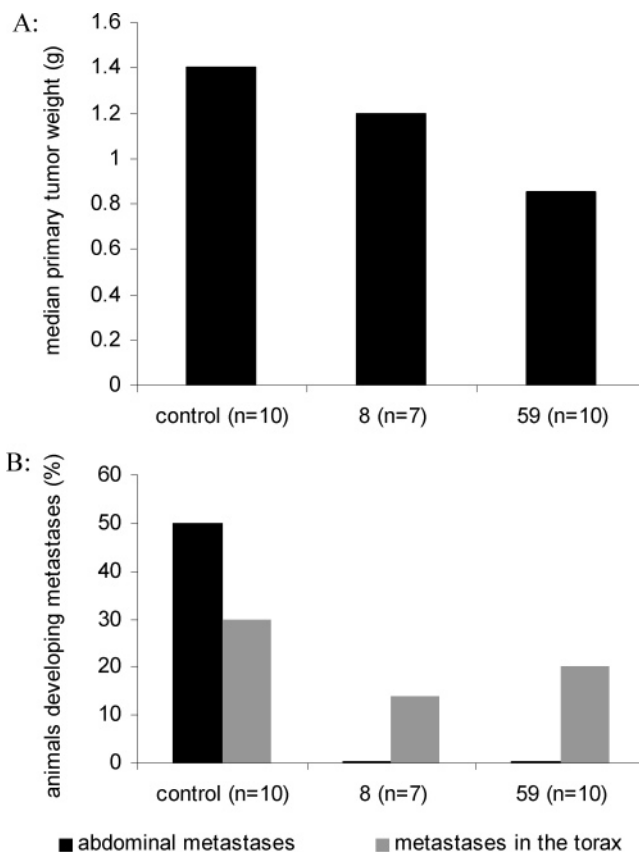


Figure 2. Effect of the matriptase inhibitors **8** and **59** on median primary tumor growth (A) and the metastatic potential (B) of PC-3-derived tumors in an orthotopic mouse model of pancreatic cancer. The inhibitors were administered intraperitoneally at a daily dose of 5 mg/kg for 4 weeks into nude mice with orthotopically transplanted PC-3-derived tumors. Abdominal metastases (black) were only found in the vehicle-treated control group but not in the treatment groups. The dissemination into the thorax (gray) was reduced by 53% and 33% for inhibitors **8** and **59**, respectively. Three mice treated with inhibitor **8** died because of postoperative suffering during the first treatment days.

determined for the less selective analogues **8** and **54**, probably because of a moderate thrombin inhibition. The estimated IC₂₀₀ values in the TT, aPTT, and PT assays are 0.32, 2.7, and 3.8 μM for inhibitor **8** and 0.27, 1.5, and 1.6 μM for analogue **54**, respectively.

The potency of matriptase inhibitors **8** and **44** has previously been demonstrated in a series of in vitro assays.³² Both inhibitors are able to reduce the matriptase-catalyzed processing of pro-HGF into HGF with IC₅₀ values between 1 and 3 μM and inhibit the pro-HGF/SF-induced scattering of matriptase-expressing DLD-1 and PC-3 cells at micromolar concentrations, as well as their subsequent invasion in a matrigel assay.

Matriptase has been isolated as a major protease of the human prostate carcinoma cell line PC-3.¹⁰ Two additional recent studies showed that matriptase expression is elevated in human prostate carcinoma compared to benign prostate tissue.^{33,34} Because the protein level of matriptase increases with increasing tumor grade, matriptase was suggested to be a novel predictive biomarker for human prostate adenocarcinoma. The increase of matriptase expression comes along with a progressive loss of the expression of its cognate inhibitor, hepatocyte growth factor activator inhibitor type 1 (HAI-1), implicating that matriptase may be functionally involved in the progression of prostate cancer and giving a rationale for inhibiting matriptase in anticancer therapy. Therefore, we have studied the effects of two of our inhibitors on primary tumor growth and metastasis

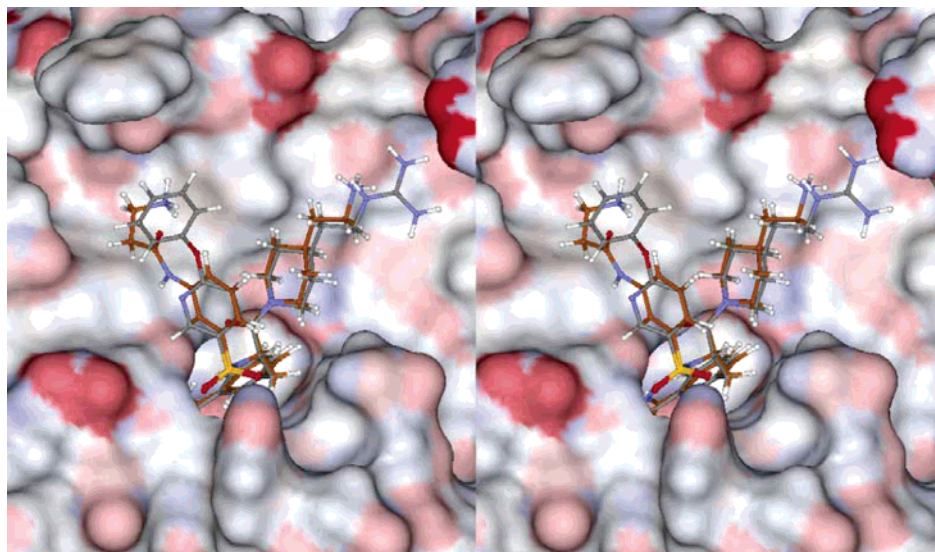


Figure 3. Models of inhibitors **54** (gray carbon atoms) and **59** (orange carbon atoms) in complex with matriptase, visualized as a surface indicating the atom charges. The compounds were manually modeled into the active site cleft of matriptase under consideration of the known interactions between the sulfonated peptidic backbone of the inhibitor and the Trp215-Gly219 segment of matriptase as well as the most probable interactions of these compounds with the S2/S4 subsite and the S1 specificity pocket, respectively. The models were generated from the X-ray structure of inhibitor **8** in matriptase by replacement of the sulfonyl substituent in both analogues and elimination of the C-terminal carbamidine in the case of compound **59**.

formation in an orthotopic xenograft model of prostate cancer using PC-3-derived tumor tissue. The compounds were well tolerated and inhibited both the primary growth and the metastatic capacity of these tumors. These results confirm a previously published study with an arginal-derived matriptase inhibitor, which inhibited the growth of tumors established from human androgen independent prostate cell lines CWR22R and CWRSA6.¹⁸ Also in this study, no side effects due to matriptase inhibition have been described, although experiments with knockout mice have demonstrated that matriptase is required for postnatal survival, and one might argue that the inhibition of matriptase could lead to side effects *in vivo*. Matriptase exhibits its pleiotropic functions in epidermal differentiation due to profilaggrin-processing, hair follicle development, and thymic homeostasis.^{35,36} Obviously, other matriptase substrates are involved in tumor progression and invasion, such as pro-HGF and pro-uPA.

Our data provide an additional proof of concept for the targeting of matriptase in the design of new anti-invasive drugs.

Experimental Section

Synthesis. All reagents, solvents for synthesis, and amino acids were purchased from Aldrich, Lancaster, Acros, Fluka, or Bachem and were used without further purification. 3-Cyanophenylalanine was obtained from Senn Chemicals, Switzerland. The molecular mass of the inhibitors was determined using a Finnigan ESI-MS LCQ (Bremen, Germany). Analytical HPLC experiments were performed on a Shimadzu LC-10A system (Phenomenex Luna C₁₈, 5 μ m column, 4.6 mm \times 250 mm) with a linear gradient of acetonitrile (10–70% in 60 min, detection at 220 nm) containing 0.1% TFA at a flow rate of 1 mL/min. The final inhibitors were purified to more than 97% purity by preparative HPLC on a Shimadzu LC-8A system (Phenomenex Luna C₁₈, 5 μ m column, 30 mm \times 250 mm) with a linear gradient of acetonitrile (45% increase of acetonitrile within 120 min, detection at 220 nm) containing 0.1% TFA at a flow rate of 10 mL/min and obtained as TFA salts after lyophilization. Thin-layer chromatography was performed on silica gel plates (silica gel 60 F₂₅₄, Merck, Darmstadt, Germany) in *n*-butanol/acetic acid/water 4/1/1 (v/v/v). ¹H NMR spectra were recorded on a Bruker DPX-300 spectrometer at 300.13 MHz, and chemical shifts are referenced to the residual proton signal of the solvent.

2-Naphthylsulfonyl-3-acetyloxamidinophenylalanine (2-Nas-Phe(3-AcOxam)-OH) (3). An amount of 3.8 g (10 mmol) of 2-Nas-Phe(3-CN)-OH, obtained by coupling of 2-Nas-Cl to 3-cyanophenylalanine under Schotten-Baumann conditions,²⁸ was dissolved in 100 mL of absolute ethanol and treated with 1.39 g (20 mmol) of hydroxylamine-HCl and 3.48 mL (20 mmol) of DIPEA (diisopropylethylamine). The mixture was refluxed for 6 h and stirred overnight at room temperature. The solvent was evaporated. The remaining oil was dissolved in 50 mL of acetic acid and 2.83 mL (30 mmol) of acetic anhydride. The mixture was stirred at room temperature for 30 min. The solvent was evaporated, and the remaining oil was dissolved in ethyl acetate and washed 3 \times with brine. The organic layer was dried over Na₂SO₄ and evaporated. The product was crystallized from ethyl acetate/petroleum ether (bp 40–60 $^{\circ}$ C) to give a white solid (yield, 3.02 g = 6.64 mmol; TLC, *R*_f = 0.67; HPLC, retention time 34.04 min; MS 456 (M + H)⁺; ¹H NMR (DMSO-*d*₆) δ 2.13 (s, 3H), 2.70–3.05 (m, 2H), 4.01 (m, 1H), 6.68 (s, br, 2H), 7.12 (m, 1H), 7.20 (d, 1H), 7.42 (d, 1H), 7.52 (s, 1H), 7.54–7.69 (m, 3H), 7.96 (m, 2H), 8.04 (d, 1H), 8.24 (s, 1H), 8.34 (d, 1H), 12.67 (s, br, 1H).

4-(2-Aminoethyl)pyridine (4). A slurry of 76.23 g (1.42 mol) of ammonium chloride and 74.71 g (0.71 mol) of 4-vinylpyridine in 225 mL of water and 100 mL of methanol was refluxed overnight. The solution was cooled. At 0 $^{\circ}$ C, an amount of 59.02 g (1.47 mol) of NaOH was added in small portions. The aqueous layer was extracted 3 \times with chloroform, and the organic layer was dried over Na₂SO₄ and evaporated. The remaining oil was purified by distillation (22 mbar, 121 $^{\circ}$ C, oil; yield, 46.9 g = 0.38 mol; TLC, *R*_f = 0.11; MS 123 [M + H]⁺; ¹H NMR (CDCl₃) δ 0.94 (s, br, 2H), 2.53 (t, 2H), 2.78 (t, 2H), 6.90 (d, 2H), 8.30 (d, 2H)).

4-(2-Boc-amidoethyl)piperidine (5). An amount of 29.5 g (135 mmol) of di-*tert*-butyl dicarbonate, dissolved in 50 mL of *tert*-butanol, was added within 30 min to 15 g (123 mmol) of 4-(2-aminoethyl)pyridine (**4**) in 250 mL of *tert*-butanol. The mixture was stirred at room temperature for 12 h and washed twice with saturated NaHCO₃ solution and once with brine. The organic layer was dried over Na₂SO₄ and evaporated (oil, 23.9 g, 107 mmol, *R*_f = 0.43). The remaining oil was dissolved in 800 mL of 90% acetic acid and treated with 250 mg of catalyst (PtO₂). The mixture was stirred under an atmosphere of hydrogen at 35 $^{\circ}$ C for 96 h. The catalyst was removed by filtration, and the solvent was evaporated. The residue was dissolved in water adjusted to pH 11 with 1 N NaOH. The aqueous layer was extracted 3 \times with DCM. The

organic layer was dried over Na_2SO_4 , and the solvent was evaporated. The product crystallized from the remaining oil at 4 °C (white solid; yield, 21.9 g = 96 mmol; TLC, R_f = 0.38; MS 229.2 [M + H]⁺; ¹H NMR (DMSO-*d*₆): δ 1.31 (m, 4H), 1.36 (s, 9H), 1.50 (m, 1H), 1.75 (d, 2H), 2.74 (m, 2H), 2.93 (m, 2H), 3.17 (m, 2H) 6.75 (br, 1H)).

2-Nas-Phe(3-AcOxam)-4-(2-Boc-amido)ethylpiperidide (6). An amount of 500 mg (1.1 mmol) of 2-Nas-Phe(3-AcOxam)-OH (**3**) and 251 mg (1.1 mmol) of compound **5** were dissolved in 10 mL of DMF. At 0 °C 571 mg (1.1 mmol) of PyBop and 383 μL (2.2 mmol) of DIPEA were added. The mixture was stirred for 20 min at 0 °C and for an additional period of 3 h at room temperature. The solvent was evaporated, and the remaining oil was dissolved in ethyl acetate, washed 3 \times with 5% KHSO_4 solution, 1 \times with brine, 3 \times with saturated NaHCO_3 solution, and 2 \times with brine. The organic layer was dried over Na_2SO_4 , and the solvent was evaporated. The remaining brown foam was purified by preparative reversed-phase HPLC, and the product was dried in vacuo (white solid; yield, 583 mg = 0.88 mmol; TLC, R_f = 0.85; HPLC, retention time 48.07 min; MS 664.3 [M - H]⁻; ¹H NMR (CDCl_3 -*d*), two conformers in a relative ratio of 55:45, δ -0.15 (m, 1H), 0.54 (m, 0.55H), 0.64 (m, 1H), 0.98–1.25 (m, 4H), 1.37 (s, 4.05H), 1.39 (s, 4.95H), 1.50 (m, 0.45H), 2.15 (s, 3H), 2.20 (m, 2H), 2.70–2.98 (m, 4H), 3.26 (m, 1H), 3.90–4.06 (m, 1H), 4.26–4.49 (m, 1H), 5.58 (br, 2H), 6.50 (m, 1H), 7.18 (m, 2H), 7.48–7.60 (m, 4H), 7.70 (m, 1H), 7.83 (m, 3H), 8.29 (s, 1H)).

2-Nas-Phe(3-Am)-4-(2-aminoethyl)piperidide·2TFA (7). An amount of 5 mL of 1 N HCl in glacial acetic acid was added to 500 mg (0.75 mmol) of compound **6** and was dissolved in 5 mL of acetic acid. The mixture was shaken at room temperature for 1 h. The solvent was evaporated, and the remaining product (TLC: R_f = 0.35; HPLC, retention time 25.66 min; MS 566.3 [M + H]⁺) was dissolved in 50 mL of 90% acetic acid and treated with 15 mg of catalyst (10% Pd/C). The mixture was stirred under an atmosphere of hydrogen at 40 °C overnight. The catalyst was removed by filtration, and the solvent was evaporated. The crude product was purified by reversed-phase HPLC and lyophilized from water (white powder; yield, 70.4 mg = 0.096 mmol; TLC, R_f = 0.34; HPLC, retention time 19.03 min; MS 508.4 [M + H]⁺; ¹H NMR (DMSO-*d*₆), two conformers in a relative ratio of 40:60, δ -0.02 (m, 1H), 0.43 (m, 0.4H), 0.58 (m, 0.6H), 1.09–1.45 (m, 5H), 1.69 (m, 0.4H), 2.14 (m, 0.6H), 2.59–2.83 (m, 4H), 2.90 (m, 1H), 3.70 (s, br, 2H), 3.70–3.94 (m, 2H), 4.53 (m, 1H), 7.37–7.50 (m, 2H), 7.58 (d, 1H), 7.62–7.75 (m, 6H), 7.97–8.10 (m, 3H), 8.17 (d, 0.6H), 8.27 (d, 0.4H), 8.30 (s, 1H), 9.25 (s, br, 3H)).

2-Nas-Phe(3-Am)-4-(2-guanidinoethyl)piperidide·2TFA (8). An amount of 50 mg (0.068 mmol) of compound **7** was dissolved in 2 mL of DMF and treated with 20 mg (0.136 mmol) of 1*H*-pyrazole-1-carboxamidinium·HCl and 35.5 μL (0.204 mmol) of DIPEA. The mixture was stirred for 24 h, the solvent was evaporated, and the remaining crude product was purified by reversed-phase HPLC and lyophilized from water (white powder; yield, 42 mg = 0.054 mmol; TLC, R_f = 0.40; HPLC, retention time 21.19 min; MS 550.4 [M + H]⁺; ¹H NMR (DMSO-*d*₆), two conformers in a relative ratio of 40:60, δ -0.10 (m, 0.6H), 0.08 (m, 0.4H), 0.45 (m, 1H), 0.95 (m, 1H), 1.20 (m, 3H), 1.35 (m, 1H), 1.70 (m, 0.4H), 2.12 (m, 0.6H), 2.45 (m, 0.6H), 2.66 (m, 0.4H), 2.78 (m, 1H), 2.94 (m, 3H), 3.79 (m, 2H), 4.54 (m, 1H), 5.60 (s, br, 1H), 7.23 (s, br, 3H), 7.44 (m, 2H), 7.63 (m, 5H), 7.75 (s, 1H), 8.02 (m, 3H), 8.16 (d, 0.6H), 8.24 (d, 0.4H), 8.30 (d, 1H), 9.27 (s, br, 2H), 9.41 (s, br, 2H)).

3-Nitrophenylsulfonyl-Phe(3-CN)-4-(2-Boc-amido)ethylpiperidide (9). The synthesis was performed by PyBop mediated coupling as described for compound **6** using 3.9 g (10.39 mmol) of 3-nitrophenylsulfonyl-Phe(3-CN)-OH and 2.37 g (10.39 mmol) of **5** as starting materials (orange oil; yield, 5.3 g; purity 81% based on analytical HPLC at 220 nm). A sample was purified by preparative reversed-phase HPLC for analysis (TLC, R_f = 0.96; HPLC, retention time 50.34 min; MS 584.3 [M - H]⁻; ¹H NMR, (CDCl_3 -*d*), two conformers in a relative ratio of 1:1, δ 0.32 (m, 0.5H), 0.68 (m, 0.5H), 0.82 (m, 1H), 1.30 (m, 2H), 1.42 (s, 9H),

1.75 (m, 2H), 2.23 (m, 0.5H), 2.44 (m, 0.5H), 2.66 (m, 0.5H), 2.91 (m, 2.5H), 3.07 (m, 2H), 3.62 (m, 1H), 4.27 (m, 1H), 4.49 (m, 1H), 4.55 (m, 0.5H), 6.47 (m, 1H), 7.37 (m, 3H), 7.46 (m, 1H), 7.66 (m, 1H), 8.04 (m, 1H), 8.35 (m, 1H), 8.47 (m, 1H), 8.66 (broad, 1H); one resonance hidden by the large tBu signal at 1.42 ppm).

N-(3-Cbz- β -Ala)amidophenylsulfonyl-Phe(3-CN)-4-(2-Boc-amido)ethylpiperidide (10). An amount of 5 g of the crude **9** was dissolved in 100 mL of acetic acid at room temperature and treated with zinc powder. The mixture was stirred for 1.5 h, the remaining zinc was removed by filtration, and the solvent was evaporated. The residue was dissolved in ethyl acetate and washed 4 \times with saturated NaHCO_3 solution and 2 \times with brine. The organic layer was dried over Na_2SO_4 and evaporated (yellow foam; yield, 4.5 g; TLC, R_f = 0.86; HPLC, retention time 40.29 min; MS [M - H]⁻ 554.2). An amount of 2.74 g of the crude 3-aminophenylsulfonyl-Phe(3-CN)-4(2-Boc-amido)ethylpiperidide was added to a mixed anhydride, which was prepared from 1.0 g (4.48 mmol) of Cbz- β -Ala-OH, 583 μL (4.48 mmol) of isobutyl chloroformate, and 493 μL (4.48 mmol) of *N*-methylmorpholine in DMF at -15 °C within 10 min. The mixture was stirred for 1 h at -15 °C and at room temperature overnight. The solvent was evaporated, and the residue was dissolved in ethyl acetate, washed 3 \times with 5% KHSO_4 solution, 1 \times with brine, 3 \times with saturated NaHCO_3 solution, and 3 \times with brine. The organic layer was dried over Na_2SO_4 and evaporated (brown oil). The product was obtained as a TFA salt after preparative reversed-phase HPLC (white lyophilized powder; yield, 2.3 g = 3.02 mmol; TLC, R_f = 0.96; HPLC, retention time 51.88 min; MS 759.2 [M - H]⁻; ¹H NMR, (CDCl_3 -*d*), two conformers in a relative ratio of 0.62:0.38, multiplicity not assigned because of broad resonances at room temperature, δ 0.21 (1H), 0.58 (0.62H), 0.73 (0.38H), 1.21 (2H), 1.40 (3.42H), 1.41 (5.58H), 1.50 (1H), 2.17 (0.38H), 2.29 (0.62H), 2.44 (0.62H), 2.57 (2H), 2.63 (0.38H), 2.85 (2H), 2.98 (2H), 3.35 (1.38H), 3.49 (2.62H), 4.24 (1.62H), 4.41 (0.38H), 4.58 (0.38H), 4.75 (0.62H), 5.05 (2H), 5.73 (1H), 6.67 (1H), 7.23–7.45 (11.76H), 7.68 (0.62H), 7.84 (1H), 8.09 (0.62H), 8.75 (0.38H), 9.10 (0.62H)).

N-(3-Cbz- β -Ala)amidophenylsulfonyl-Phe(3-Am)-4-(2-Boc-amido)ethylpiperidide·TFA (11). The intermediate *N*-(3-Cbz- β -Ala)amidophenylsulfonyl-Phe(3-AcOxam)-4(2-Boc-amido)ethylpiperidide, prepared from 242 mg (0.318 mmol) of the nitrile **10** as described for compound **3**, was reduced with zinc powder in acetic acid over a period of 3 h at room temperature. The remaining zinc was removed by filtration, the solvent was evaporated, and the product was obtained by preparative HPLC (white lyophilized powder; yield, 121 mg = 0.135 mmol; TLC, R_f = 0.76; HPLC, retention time 36.41 min; MS 778.5 [M + H]⁺; ¹H NMR, (CDCl_3 -*d*), two conformers in a relative ratio of 1:1, multiplicity not assigned because of very broad resonances at room temperature, dilute samples also gave very broad signals, δ -0.31 (0.5H), 0.39 (0.5H), 0.62 (1H), 1.21 (2H), 1.41 (9H), 2.15 (2H), 2.33 (0.5H), 2.61 (3H), 2.88 (4H), 3.49 (3H), 4.04 (0.5H), 4.22 (1H), 4.31 (0.5H), 4.52 (0.5H), 5.02 (2H), 5.87 (0.5H), 6.01 (0.5H), 7.25 (10H), 7.65 (3H), 8.03 (1H), 8.23 (1H), 8.53 (1H), 9.38 (0.5H), 9.54 (0.5H), 10.00 (1H), 10.07 (1H)).

N-(3- β -Ala)amidophenylsulfonyl-Phe(3-Am)-4-(2-guanidino)ethylpiperidide·3TFA (12). An amount of 120 mg of compound **11** was dissolved in 3 mL of 90% TFA and shaken for 1 h at room temperature. The solvent was evaporated and lyophilized from water (124 mg; TLC, R_f = 0.27; HPLC, retention time 21.76 min; MS 678.3 [M + H]⁺). An amount of 120 mg (0.132 mmol) of the TFA salt was dissolved in 2 mL of DMF and treated with 38.7 mg (0.264 mmol) of 1*H*-pyrazole-1-carboxamidinium·HCl and 69 μL (0.396 mmol) of DIPEA. The mixture was stirred for 24 h. The solvent was evaporated, and the remaining oil (TLC, R_f = 0.36; HPLC, retention time 23.04 min; MS 720.3 [M + H]⁺) was dissolved in 50 mL of 90% acetic acid and treated with 10 mg of catalyst (10% Pd/C). The mixture was hydrogenated at room temperature overnight. The catalyst was removed by filtration, the solvent was evaporated, and the product was purified by reversed-phase HPLC and lyophilized from water (white powder; yield, 48 mg = 0.052 mmol; TLC, R_f = 0.04; HPLC, retention time 10.38 min; MS 586.3

[M + H]⁺; ¹H NMR (D₂O-*d*₂), two conformers in a relative ratio of 0.54:0.46, δ 0.07 (m, 0.46H), 0.69 (m, 1.54H), 1.35 (m, 1H), 1.45 (m, 1H), 1.50 (m, 1H), 1.62 (m, 2H), 2.24 (m, 0.46H), 2.54 (m, 0.54H), 2.77 (m, 1H), 2.95 (m, 2.46H), 3.08 (m, 1.54H), 3.15 (m, 1H), 3.21 (m, 1H), 3.41 (m, 2H), 3.73 (m, 1H), 4.06 (m, 1H), 4.56 (m, 1H), 7.57 (m, 5H), 7.71 (m, 2H), 7.96 (m, 1H)).

Cloning of the Serine Protease Domain of Matriptase. The serine protease domain was amplified from I.M.A.G.E. clone IMAGp998N139560 (RZPD, Berlin, Germany) by PCR using 5'-GGCAATTCCATATGAAACATCACCATCATCACCATGT-TGTTGGGGGCACGGATGCG-3' and 5'-GCATGAATTCTTA-TACCCAGTGTCTCTTTGATCCA-3' as sense and antisense primers, respectively. The primers were chosen to introduce an NdeI site at the 5' end of the protease domain followed by a MK(His)₆ sequence and an EcoRI site at the 3' end of matriptase. The ~750 base pair long amplification product was purified, digested with NdeI and EcoRI, and subcloned into pET24 (Novagen, Merck Biosciences, Bad Soden, Germany) for expression in *Escherichia coli*. The catalytic domain of matriptase was expressed in inclusion bodies and then subsequently denatured, purified, refolded, and activated as described below.

Expression, Purification, Refolding, and Activation of the Catalytic Domain of Matriptase. BL21(DE3) cells (Novagen) containing the expression vector were incubated in LB and 30 μ g/mL kanamycin at 37 °C and 250 rpm. The expression was induced by the addition of 1 mM IPTG at a cell density of OD₆₀₀ = 0.8, and the incubation continued for 1 h. The cells were harvested and lysed with BugBuster protein extraction reagent (Novagen), and the DNA was digested with Benzonase (25 U/g cell pellet, Novagen). The inclusion bodies were washed and denatured with denaturation buffer (6 M guanidine HCl, 10 mM Tris-HCl, 100 mM sodium phosphate, pH 8.0, 5 mL per 1 mL of pellet). The denatured protein was freed from insoluble constituents by centrifugation and filtration (0.2 μ m), and the his-tagged matriptase was purified by metal chelate chromatography (NiNTA Agarose, Qiagen, Hilden, Germany). Matriptase-containing fractions were pooled, derivatized with glutathione, and then renatured by dilution to a final protein concentration of 50 μ g/mL in refolding buffer (50 mM Tris-HCl, 0.5 M L-arginine, 20 mM CaCl₂, 1 mM EDTA, 0.1 M NaCl, 1 mM cysteine, pH 7.5). After 3 days of incubation at room temperature, the refolding solution was filtered and concentrated to >300 μ g/mL by ultrafiltration (Centricon Plus-80, PL-10, Millipore, Schwabach, Germany) and the buffer was exchanged to activation buffer (20 mM sodium phosphate, 150 mM NaCl, pH 7.0).

Because correct processing of the N-terminus is required for the activity of serine proteases, the refolded matriptase had to be activated by removal of the N-terminal peptide sequence MK(His)₆. This was achieved by incubating the protease for 2 h with 2.5 mU/mL of activated DAPase (Qiagen) and by subsequent separation of activated from nonactivated matriptase and his-tagged DAPase via metal chelate chromatography. The yield of this procedure was approximately 2 mg of active catalytic domain per 1 L of culture.

Enzyme Kinetics. The kinetic measurements with thrombin, factor Xa, uPA, and plasmin were performed as described previously.²⁸ The matriptase activity was determined at 405 nM using the chromogenic substrate Pefachrome tPA (Loxo GmbH, Dossenheim, Germany) in 0.05 M Tris-HCl buffer, pH 8.0, containing 0.154 M NaCl, 0.1% BSA, and 5% (v/v) ethanol.

Animal Study. An orthotopic xenograft mouse model of prostate cancer was performed by Oncotest GmbH (Freiburg, Germany) according to the guidelines of the German Animal Health and Welfare Act. Small tumor fragments of 0.5–1 mm in diameter that had been established by subcutaneous inoculation of the human prostate tumor cell line PC3 in nude mice were orthotopically transplanted into 5-week-old to 6-week-old male anesthetized NMRI nu/nu mice. After an induction period of 4 days that also allowed healing of the surgery wound, treatment of the established tumors was started. Animals were randomized into groups of 7–10 tumor-bearing mice and intraperitoneally treated daily, 7 days a week, with inhibitor **8** or **59** (5 mg/kg/day) or vehicle (0.9% saline),

Table 5. Refinement Statistics for the Matriptase Complexes with Inhibitors **8** and **31** Determined by X-ray Crystallography

parameter	8	31
resolution range (Å)	14.6–2.1	14.6–2.2
space group	C222	C222
molecules per asymmetric unit	1	1
<i>a</i> (Å)	66.84	67.07
<i>b</i> (Å)	141.02	140.15
<i>c</i> (Å)	51.80	51.73
α, β, γ (deg)	90, 90, 90	90, 90, 90
no. of reflections	59, 899	85, 118
completeness (%)	99.3	98.0
multiplicity	4.1	3.7
<i>R</i> _{merge} (%)	10.6	15.8
no. of unique reflections	14,540	12,728
<i>R</i> _{fac} (%)	18.19	19.69
<i>R</i> _{free} (%) (test set, %)	22.93 (4.9)	23.87 (5.1)
rmsd bonds (Å)	0.008	0.008

respectively. After a treatment period of 4 weeks, animals were sacrificed and the antitumor activity was determined as tumor weight relative to the tumors in the vehicle control group. The antimetastatic capacity was determined by macroscopic determination of metastases during a pathological examination.

X-ray Analysis. Structure determination and crystallographic refinement were performed as described previously.¹¹ Briefly, platelike crystals of the benzamidine–matriptase complex were grown at 18 °C from a solution containing 5 mg/mL matriptase, 10 mM benzamidine, 0.1 M Tris-HCl, pH 8.5, 20% PEG 8000, and 200 mM MgCl₂, using the hanging drop vapor diffusion technique. These crystals were transferred to the same buffer lacking benzamidine and containing 1 mM of compound **8** or **31**. After soaking for 3 h, the crystals were transferred to the same buffer containing 16% glycerol and were flash-frozen in a nitrogen stream of 100 K.

Complete data sets to 2.1 and 2.2 Å resolution were collected in-house using a 345 mm MAR Research image plate (MAR Research, Norderstedt, Germany) and monochromatic Cu K α radiation from a RIGAKU rotating anode X-ray generator (Rigaku/MSK, Sevenoaks, U.K.). The data were evaluated with the MOSFLM package³⁷ and scaled using SCALA from the CCP4 program suite³⁸ (see Table 5). Starting with the matriptase coordinates 1eax, the structures were crystallographically refined using CNS, version 1.1.³⁹ In between, the inhibitor compounds were built with Sybyl 7.0 (Tripos, Inc.) and placed into the appropriate electron density using MAIN.⁴⁰ In the final rounds of refinement, water molecules were added and individual restrained atomic *B* values were refined. The *R*_{free} was calculated from 5.0% of the reflections not used for refinement. The final *R*_{fac}/*R*_{free} values are 18.2/23.0 and 19.7/23.9% (see Table 5).

Acknowledgment. The authors thank Ute Altmann, Rainer Sieber, Angelika Grau, Claudia Neuwirth, Cathleen Naumann, and Martin Korsonewski for their excellent technical help. The authors also thank Chris Privalle for correcting the English version of the manuscript. This work was supported by the Thuringian Ministry of Economy, Technology and Labor (TMWTA).

Supporting Information Available: A table containing MS and HPLC data of all final inhibitors and ¹³C NMR spectra of compounds described in the Experimental Section of the manuscript. This material is available free of charge via the Internet at <http://pubs.acs.org>.

References

- Coussens, L. M.; Fingleton, B.; Matrisian, L. M. Matrix metalloproteinase inhibitors and cancer: Trials and tribulations. *Science* **2002**, *295*, 2387–2392.
- Rockway, T. W.; Nienaber, V.; Giranda, V. L. Inhibitors of the protease domain of urokinase-type plasminogen activator. *Curr. Pharm. Des.* **2002**, *8*, 2541–2558.

- (3) Steinmetzer, T. Synthetic urokinase inhibitors as potential antitumor drugs. *IDrugs* **2003**, *6*, 137–145.
- (4) Hopper, J. D.; Clements, J. A.; Quigley, J. P.; Antalis, T. M. Type II transmembrane serine proteases. *J. Biol. Chem.* **2001**, *276*, 857–860.
- (5) Takeuchi, T.; Harris, J. L.; Huang, W.; Yan, K. W.; Coughlin, S. R.; Craik, C. S. Cellular localization of membrane-type serine protease 1 and identification of protease-activated receptor-2 and single-chain urokinase-type plasminogen activator as substrates. *J. Biol. Chem.* **2000**, *275*, 26333–26342.
- (6) Lee, S.-L.; Dickson, R. E.; Lin, C.-Y. Activation of hepatocyte growth factor and urokinase/plasminogen activator by matriptase, an epithelial membrane serine protease. *J. Biol. Chem.* **2000**, *275*, 36720–36725.
- (7) Shi, Y. E.; Torri, J.; Yieh, L.; Wellstein, A.; Lippman, M. E.; Dickson, R. B. Identification and characterization of a novel matrix-degrading protease from hormone-dependent human breast cancer cells. *Cancer Res.* **1993**, *53*, 1409–1415.
- (8) Lin, C.-Y.; Wang, J.-K.; Torri, J.; Dou, L.; Sang, Q. A.; Dickson, R. B. Characterization of a novel, membrane-bound, 80-kDa matrix-degrading protease from human breast cancer cells. *J. Biol. Chem.* **1997**, *272*, 9147–9152.
- (9) Lin, C.-Y.; Anders, J.; Johnson, M.; Dickson, R. B. Purification and characterization of a complex containing matriptase and a kunitz-type serine protease inhibitor from human milk. *J. Biol. Chem.* **1999**, *274*, 18237–18242.
- (10) Takeuchi, T.; Shuman, M. A.; Craik, C. A. Reverse biochemistry: Use of macromolecular protease inhibitors to dissect complex biological processes and identify a membrane-type serine protease in epithelial cancer and normal tissue. *Proc. Natl. Acad. Sci. U.S.A.* **1999**, *96*, 11054–11061.
- (11) Friedrich, R.; Fuentes-Prior, P.; Ong, E.; Coombs, G.; Hunter, M.; Oehler, R.; Pierson, D.; Gonzalez, R.; Huber, R.; Bode, W.; Madison, E. Catalytic domain structures of MT-SP1/matriptase, a matrix-degrading transmembrane serine proteinase. *J. Biol. Chem.* **2002**, *277*, 2160–2168.
- (12) Oberst, M. D.; Johnson, M. D.; Dickson, R. B.; Lin, C.-Y. Singh, B.; Stewart, M.; Williams, A.; al-Nafussi, A.; Smyth, J. F.; Gabra, H.; Sellar, G. C. Expression of the serine protease matriptase and its inhibitor HAI-1 in epithelial ovarian cancer: Correlation with clinical outcome and tumor clinicopathological parameters. *Clin. Cancer Res.* **2002**, *8*, 1101–1107.
- (13) Bhatt, A. S.; Takeuchi, T.; Yistra, B.; Ginzinger, D.; Albertson, D.; Shuman, M. A.; Craik, C. S. Quantification of membrane type serine protease 1 (MT-SP1) in transformed and normal cells. *Biol. Chem.* **2003**, *384*, 257–266.
- (14) Hoang, C. D.; D’Cunha, J. D.; Kratzke, M. G.; Casmeay, C. E.; Frizelle, S. P.; Maddaus, M. A.; Kratzke, R. A. Gene expression profiling identifies matriptase overexpression in malignant mesothelioma. *Chest* **2004**, *125*, 1843–1852.
- (15) List, K.; Szabo, R.; Molinolo, A.; Sriuranpong, V.; Redeye, V.; Murdock, T.; Burke, B.; Nielson, B. S.; Gutkind, J. S.; Bugge, T. H. Deregulated matriptase causes ras-independent multistage carcinogenesis and promotes ras-mediated malignant transformation. *Genes Dev.* **2005**, *19*, 1934–1950.
- (16) Enyedy, I.; Lee, S.-L.; Kuo, A. H.; Dickson, R. B.; Lin, C.-Y.; Wang, S. Structure-based approach for the discovery of bis-benzamides as novel inhibitors of matriptase. *J. Med. Chem.* **2001**, *44*, 1349–1355.
- (17) Long, Y.-Q.; Lee, S.-L.; Lin, C.-Y.; Enyedy, I.; Wang, S.; Li, P.; Dickson, R. B.; Roller, P. P. Synthesis and evaluation of the sunflower derived trypsin inhibitor as a potent inhibitor of the type II transmembrane serine protease, matriptase. *Bioorg. Med. Chem. Lett.* **2001**, *11*, 2515–2519.
- (18) Galkin, A. V.; Mullen, L.; Fox, W. D.; Brown, J.; Duncan, D.; Moreno, O.; Madison, E. L.; Agus, D. B. CVS-3983, a selective matriptase inhibitor, suppresses the growth of androgen independent prostate tumor xenografts. *Prostate* **2004**, *61*, 228–235.
- (19) Markwardt, F.; Wagner, G.; Stürzebecher, J.; Walsmann, P. N Alpha-arylsulfonyl-omega-(4-amidinophenyl)-alpha-aminoalkylcarboxylic acid amides. Novel selective inhibitors of thrombin. *Thromb. Res.* **1980**, *17*, 425–431.
- (20) Stürzebecher, J.; Vieweg, H.; Steinmetzer, T.; Schweinitz, A.; Stubbs, M. T.; Renatus, M.; Wikström, P. 3-Amidinophenylalanine-based inhibitors of urokinase. *Bioorg. Med. Chem. Lett.* **1999**, *9*, 3147–3152.
- (21) Judkins, B. D.; Allen, G. D.; Cook, T. A.; Evans, B.; Sardharwala, T. S. A versatile synthesis of amidines from nitriles via amidoximes. *Synth. Commun.* **1996**, *26*, 4351–4367.
- (22) Kirchner, F. K.; McCormick, J. R.; Cavallito, C. J.; Miller, L. C. The use of diazo compounds in the preparation of some benzylpenicillin esters. *J. Org. Chem.* **1949**, *14*, 388–393.
- (23) Phillips, A. P. Synthetic hypotensive agents. V. 4-(2'-Aminoethyl)-piperidine derivatives. *J. Am. Chem. Soc.* **1957**, *79*, 2836–2838.
- (24) Bernatowicz, M. S.; Wu, Y.; Matsueda, G. R. 1H-Pyrazole-1-carboxamide hydrochloride: An attractive reagent for guanylation of amines and its application to peptide synthesis. *J. Org. Chem.* **1992**, *57*, 2497–2502.
- (25) Zeslowska, E.; Schweinitz, A.; Karcher, A.; Sondermann, P.; Sperl, S.; Stürzebecher, J.; Jacob, U. Crystals of the urokinase type plasminogen activator variant beta(c)-uPA in complex with small molecule inhibitors open the way towards structure-based drug design. *J. Mol. Biol.* **2000**, *301*, 465–475.
- (26) Setyono-Han, B.; Stürzebecher, J.; Schmalix, W. A.; Muehlenweg, B.; Sieuwerts, A. M.; Timmermanns, M.; Magdolen, V.; Schmitt, M.; Klijn, J. G. M.; Foekens, J. A. Suppression of rat breast cancer metastasis and reduction of primary tumour growth by the small synthetic urokinase inhibitor WX-UK1. *Thromb. Haemostasis* **2005**, *93*, 779–786.
- (27) Stürzebecher, J.; Prasa, D.; Wikström, P.; Vieweg, H. Structure-activity relationships of inhibitors derived from 3-amidinophenylalanine. *J. Enzyme Inhib.* **1995**, *9*, 87–99.
- (28) Stürzebecher, J.; Prasa, D.; Hauptmann, J.; Vieweg, H.; Wikström, P. Synthesis and structure-activity relationships of potent thrombin inhibitors: Piperazides of 3-amidinophenylalanine. *J. Med. Chem.* **1997**, *40*, 3091–3099.
- (29) Bergner, A.; Bauer, M.; Brandstetter, H.; Stürzebecher, J.; Bode, W. The X-ray structure of thrombin in complex with N α -2-naphthyl-sulfonyl-1-3-amidino-phenylalanine-4-methylpiperidide: The beneficial effect of filling out an empty cavity. *J. Enzyme Inhib.* **1995**, *9*, 101–110.
- (30) Renatus, M.; Bode, W.; Huber, R.; Stürzebecher, J.; Stubbs, M. T. Structural and functional analyses of benzamidine-based inhibitors in complex with trypsin: Implications for the inhibition of factor Xa, tPA, and urokinase. *J. Med. Chem.* **1998**, *41*, 5445–5456.
- (31) Turk, D.; Stürzebecher, J.; Bode, W. Geometry of binding of the N alpha-tosylated piperidides of m-amidino-, p-amidino- and p-guanidino phenylalanine to thrombin and trypsin. X-ray crystal structures of their trypsin complexes and modeling of their thrombin complexes. *FEBS Lett.* **1991**, *287*, 133–138.
- (32) Förbs, D.; Thiel, S.; Stella, M. C.; Stürzebecher, A.; Schweinitz, A.; Steinmetzer, T.; Stürzebecher, J.; Uhland, K. In vitro inhibition of matriptase prevents invasive growth of cell lines of prostate and colon carcinoma. *Int. J. Oncol.* **2005**, *27*, 1061–1070.
- (33) Riddick, A. C. P.; Shukla, C. J.; Pennington, C. J.; Bass, R.; Nuttall, R. K.; Hogan, A.; Sethia, K. K.; Ellis, V.; Collins, A. T.; Maitland, N. J.; Ball, R. Y.; Edwards, D. R. Identification of degradome components associated with prostate cancer progression by expression analysis of human prostatic tissues. *Br. J. Cancer* **2005**, *92*, 2171–2180.
- (34) Saleem, M.; Adhami, V. M.; Zong, W.; Longley, B. J.; Lin, C.-Y.; Dickson, R. B.; Reagan-Shaw, S.; Jarrad, D. F. Mukhtar, H. A novel biomarker for staging human prostate adenocarcinoma: Overexpression of matriptase with concomitant loss of its inhibitor, hepatocyte growth factor activator inhibitor-1. *Cancer Epidemiol., Biomarkers Prev.* **2006**, *15*, 217–227.
- (35) List, K.; Haudenschild, C. C.; Szabo, R.; Chen, W.; Wahl, S. M.; Swaim, W.; Engelhol, L. H.; Behrendt, N.; Bugge, T. H. Matriptase/MT-SP1 is required for postnatal survival, epidermal barrier function, hair follicle development, and thymic homeostasis. *Oncogene* **2002**, *21*, 3765–3779.
- (36) List, K.; Szabo, R.; Wertz, P. W.; Segre, J.; Haudenschild, C. C.; Kim, S.-Y.; Bugge, T. H. Loss of proteolytically processed filaggrin caused by epidermal deletion of matriptase/MT-SP1. *J. Cell Biol.* **2003**, *163*, 901–910.
- (37) Leslie A. G. W. Molecular data processing. In *Crystallographic Computing 5*; Moras, D., Podjarny, A. D., Thierry, J. C., Eds.; Oxford University Press: Oxford, U.K., 1991; pp 50–61.
- (38) Collaborative Computational Project, Number 4. The CCP4 suite: programs for protein crystallography. *Acta Crystallogr.* **1994**, *D50*, 760–763.
- (39) Brünger, A. T.; Adams, P. D.; Clore, G. M.; DeLano, W. L.; Gros, P.; Grosse-Kunstleve, R. W.; Jiang, J. S.; Kuszewski, J.; Nilges, M.; Pannu, N. S.; Read, R. J.; Rice, L. M.; Simonson, T.; Warren, G. L. Crystallography & NMR system: A new software suite for macromolecular structure determination. *Acta Crystallogr.* **1998**, *D54*, 905–921.
- (40) Turk, D. Weiterentwicklung eines Programmes für Molekülgraphik und Elektronendichte-Manipulation und seine Anwendung auf verschiedene Protein-Strukturaufklärung (Advancement of a program for molecular graphics and electron density manipulation and its application to different protein structures). Ph.D. Thesis, Technische Universität München, Germany, 1992.